

Natural Products

How to cite:

International Edition: doi.org/10.1002/anie.202300773

German Edition: doi.org/10.1002/ange.202300773

Tricrilactones A–H, Potent Antiosteoporosis Macrolides with Distinctive Ring Skeletons from *Trichocladium crispatum*, an Alpine Moss-Associated Fungus

Wen-Bo Han^{+,*} Yi-Jie Zhai⁺, Rong Zhang, Xu-Shun Gong, Jia-Qian Li, Gong Xu,^{*} Xinxiang Lei, Liangcheng Du, and Jin-Ming Gao^{*}

Abstract: Tricrilactones A–H (**1–8**), a new family of oligomeric 10-membered macrolides featuring collectively five unique ring skeletons, were isolated from a hitherto unexplored fungus, *Trichocladium crispatum*. Compounds **1** and **7** contain two unconventional bridged (aza)tricyclic core skeletons, **2**, **3**, **5**, and **6** share an undescribed tetracyclic 9/5/6/6 ring system, **4** bears an uncommon 9/5/6/10/3-fused pentacyclic architecture, and **8** is a dimer bridged by an unexpected C–C linkage. Their structures, including absolute configurations, were elucidated by spectroscopic analysis, quantum chemical calculations, and X-ray diffraction analysis. Importantly, the absolute configuration of the highly flexible side chain of **1** was resolved by the asymmetric synthesis of its four stereoisomers. The intermediate-trapping and isotope labeling experiments facilitated the proposal of the biosynthetic pathway for these macrolides. In addition, their antiosteoporosis effects were evaluated in vivo (zebrafish).

Introduction

Osteoporosis is a systemic skeletal disease featured by diminished bone mass and microarchitectural deterioration in bone tissue, leading to an increased risk of bone fragility and fracture.^[1] With the growing aging population, osteoporosis has become one of the most serious and prevalent health problems worldwide.^[2] It has been estimated that approximately 200 million people are living with osteoporosis,^[3] which causes an overwhelming social burden arising from the high costs of osteoporosis care.^[4] Current strategies for osteoporosis therapy include calcium admin-

istration, vitamin supplement, and estrogen receptor modulation, as well as medical treatments (e.g. bisphosphonates and denosumab).^[5] Nevertheless, most of the targeted therapies have limitations due to their serious adverse effects, such as stroke, musculoskeletal pain, nausea, hypercalcemia, and so forth.^[2,5] Therefore, exploring a new generation of antiosteoporosis drugs with high efficacy but few side effects remains an urgent need.

Macrolides, especially the medium-sized-ring lactones (8- to 11-membered) have attracted continuous attentions of pharmacologists and chemists due to their synthetic challenges and promising bioactivities.^[6] Among them, the 10-membered macrocyclic lactones represent a large group of secondary metabolites mainly originating from fungi, as exemplified by the family of decarestrictines.^[7] The chemical dimerization is frequently encountered in microbial natural products capable of generating high structural complexity or significant bioactivities.^[8] However, dimers derived from the 10-membered lactones have hitherto remained rarely discovered, except for the only two cases of thioiscephalosporolide A^[9] and cordycicadins A–D.^[10] The medicinal value of some dimeric natural products has been showcased by the marketed drugs, such as antiviral podophyllotoxin, antineoplastic himastatin, and antidepressant hypericin.^[8]

Encouraged by these observations, we have recently identified several structurally intriguing homo- and heterodimers from fungi.^[11] To continue our pursuit of these interesting architectures, we investigated a previously unexplored fungal species, *Trichocladium crispatum* associated with the Alpine moss, by using the molecular networking guided separation (Figure S1). The investigation resulted in the characterization of eight undescribed oligomeric 10-membered macrolides, named tricrilactones A–H (**1–8**) (Figure 1). The compounds feature five new types of ring skeletons. Notably, compound **1** represents the first example

[*] Prof. W.-B. Han,⁺ Y.-J. Zhai,⁺ R. Zhang, Prof. J.-M. Gao
Shaanxi Key Laboratory of Natural Products & Chemical Biology,
College of Chemistry and Pharmacy, Northwest A&F University
Xian Yang Shi, Yangling 712100 (China)
E-mail: wbhan@nwfau.edu.cn
jinminggao@nwsuaf.edu.cn

X.-S. Gong, Prof. G. Xu
College of Plant Protection, Northwest A&F University
Xian Yang Shi, Yangling 712100 (China)
E-mail: gongxu@nwfau.edu.cn

J.-Q. Li, Prof. X. Lei
School of Pharmaceutical Sciences, South-Central Minzu University
Wuhan 430074 (China)

Prof. L. Du
Department of Chemistry, University of Nebraska-Lincoln
Lincoln, NE 68588-0304 (USA)

[†] These authors contributed equally to this work.

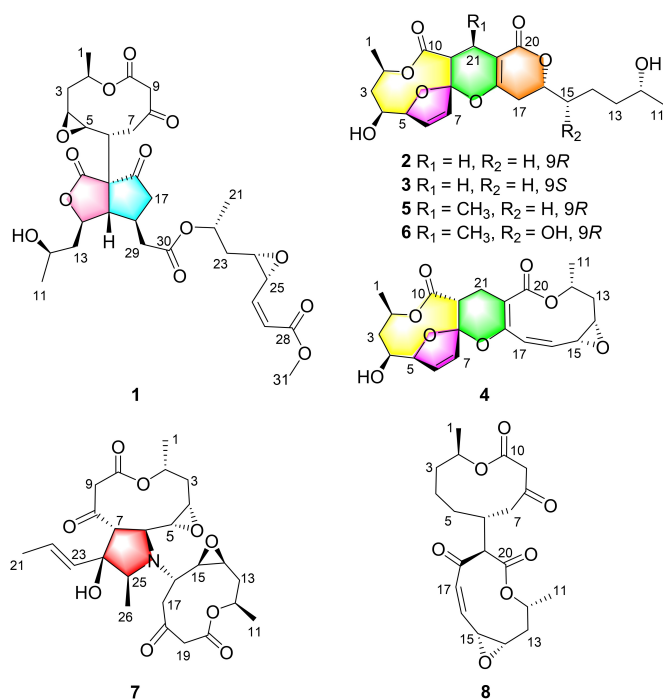


Figure 1. Chemical structures of tricrilactones A–H (1–8).

of 10-membered macrolide (pseudo)trimers bearing a bridged tricyclic core skeleton. The heterodimers **2**, **3** and **5**, **6** share an undescribed tetracyclic 9/5/6/6 skeleton harboring an unusual 1,5-dioxonan-2-one motif, whereas the structurally related homodimer **4** possesses a 9/5/6/10/3-fused pentacyclic ring skeleton. Moreover, the polyketide-alkaloid hybrid scaffold **7** represents a new class of bridged azatricyclic architectures characterized by an unconventional pyrrolidine nucleus, and compound **8** is constructed by two individual nonanolide units through an unexpected C6–C19 linkage.

Results and Discussion

Tricrilactone A (**1**), a colorless oil, has a molecular formula of C₃₁H₄₀O₁₃ according to its Na⁺-liganded molecular ion at *m/z* 643.2364 (calcd for C₃₁H₄₀O₁₃Na, 643.2361) in its high-resolution electrospray ionization mass spectrometry (HR-ESI-MS). The molecular formula was substantiated by its ¹H and ¹³C NMR spectra, which highlighted the presence of one methoxy, three methyl, seven methylene, and 11 methine groups, one quaternary carbon atom, two olefinic carbon atoms, four ester motifs and two ketones (Table S2). These substructures directly accounted for 7 of 12 double-bond equivalents, indicating that **1** was pentacyclic. Subsequently, a suite of COSY correlations of H₃-1/H-2/H₂-3/H-4/H-5/H-6/H₂-7, as well as the HMBC correlations of H-2 with C10, of H-6 with C8, of H-7 with C9, and of H₂-9 with C10 indicated a 10-membered lactone core (C1–C10), which was decorated by a *cis*-oriented 4,5-epoxide according to the large vicinal coupling constant (4.0 Hz) between H-4 and H-5.^[12] (Fig-

ure 2A, substructure **1a**). In the COSY spectrum, an additional continuous spin-system involving the correlations of H₃-11/H-12/H₂-13/H-14/H-15/H-16/H₂-17, together with the HMBC correlations of H-14 with C16 and C20, of H-15 with C20, of H-16 with C18 and C30, and of H₂-17 with C15, C19 and C29 identified an unusual tetrahydro-1*H*-cyclopenta-[c]furan-1,6(3*H*)-dione nucleus (C14–C20), which was actually edited by an isopropanol group at C14, and an acetate motif at C16, respectively (Figure 2A, substructure **1b**). In addition, a pair of mutually coupling multiplets at δ_H 3.33 (dt, *J* = 7.7, 4.5 Hz) and 4.45 (ddd, *J* = 7.5, 4.5, 0.9 Hz) unveiled a *cis*-1,2-disubstituted epoxy unit, which was assumed to be tethered by a 2-oxygenated propane residue and a 3-substituted methyl acrylate moiety, respectively, leading to the construction of a methyl (*Z*)-3-(3-propyloxiran-2-yl)acrylate fragment (C21–C28, *J*_{H26,H27} = 11.7 Hz), which was next elucidated by the COSY correlations of H₃-21/H-22/H₂-23/H-24/H-25/H-26/H-27, in combination with the HMBC correlations of H₃-21 with C23, of H-22 with C24, of H-24 with C26, of H-25 with C27, of H-26 with C28, and of H₃-31 with C28 (Figure 2A, substructure **1c**). Scrutiny of the HMBC correlations of H-5 with C19, of H-6 with C15, C18 (δ 208.2) and C20 (δ 171.2), and of H₂-7 to C19,

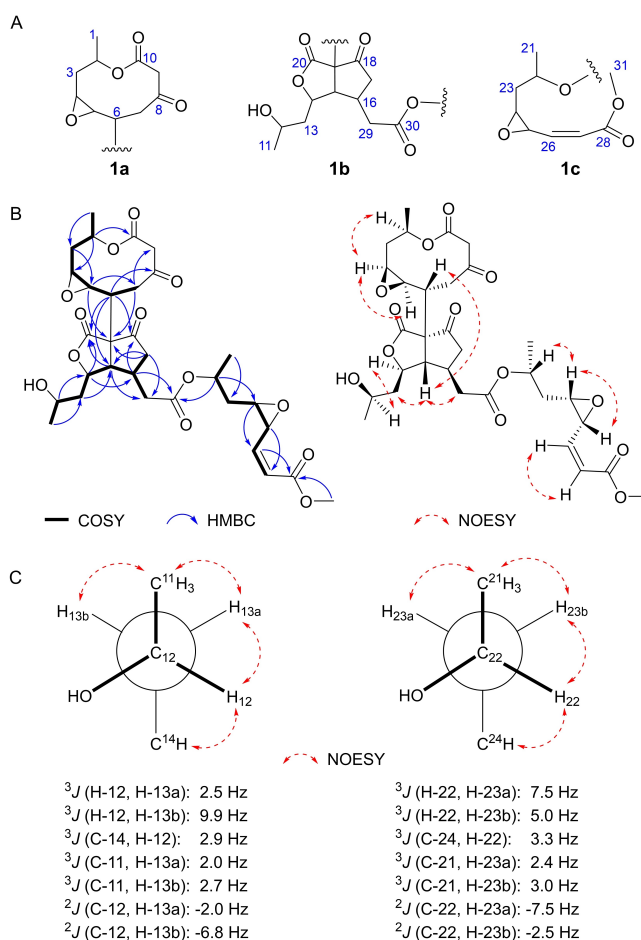


Figure 2. Structure elucidation of **1**. A) Substructures **1a**–**1c**. B) COSY, HMBC and NOE correlations. C) *J*-based configuration analysis of C12 and C22.

coupled with the HMBC correlations of H-16 with C30, of H-15 with C29, and of H-22 with C30 (δ 170.9), unambiguously established the gross structure of **1** (Figure 2B), representing a new type of „trimer-like“ macrolides harboring a unique bridged tricyclic core skeleton flanked by an embellished methyl (*Z*)-2-octenoate motif.

The relative configuration of tririlactone A (**1**) was determined by interpretation of NMR data, including NOE correlations and *J*-based configurational analysis. The NOE interactions of H-2 with H-4, and H-4 with H-5 indicated that H-2, H-4 and H-5 were on the same side (Figure 2B), while H-6 was on the opposite side of the nonanolide ring, owing to a large coupling constant (9.6 Hz) between H-5 and H-6 (Table S2). The observed NOE correlations of H-6 with H-15, and of H-15 with H₂-13 and H₂-29 positioned three residues containing nonanolide, isopropanol and acetate on the same side of the hexahydro-1*H*-cyclopenta-[*c*]furan ring system (Figure 2B). Nevertheless, the NOESY spectrum of **1** failed to confirm the relative configuration at C12 and C22, because each of them was located on a flexible side chain. Therefore, the long-range ¹³C–¹H coupling constants were measured by NMR spectroscopy based on heteronuclear couplings from aSSCI-domain experiments with e.COSY-type cross-peaks (HECADE).^[13] The small ³*J*_{H12,H13a} (2.5 Hz), ³*J*_{C11,H13a} (2.0 Hz), ³*J*_{C11,H13b} (2.7 Hz) values indicated *gauche* relationships for H-12 and H-13a, for H-13a and H₃-11, and for H₃-11 and H-13b, whereas the large ²*J*_{C12,H13b} (−6.8 Hz) value revealed the *gauche* orientation between H-13b and 12-OH. Moreover, the ²*J*_{C14,H12} (2.9 Hz) value and the NOE correlation of H-12 with H-14, as well as the correlations of H-12 with H-13a, of H₃-11 with H-13a, and of H₃-11 with H-13b led to the selective rotamer depicted in Figure 2C, thus proposing 12*R** configuration. Next, the 22*R** configuration was also verified by a similar analysis (Figure 2C).

Residual dipolar couplings (RDCs) provide not only global character but also local spatial information about the orientation of internuclear vectors (e.g., CH bonds), which encode the relative configuration of the structures.^[14] In our

previous study, we successfully employed RDC-based NMR spectroscopy for establishing the relative configuration of various natural products including herpotrichones A and B.^[11a] To further confirm the relative configuration of **1**, one-bond carbon-proton RDCs (¹*D*_{CH}) were measured using [¹H-¹³C]-CLIP-HSQC spectroscopy^[15] under isotropic conditions and in AAKVLFF anisotropic medium (Table S11).^[16] For the sake of simplicity of fitting, a divide and conquer strategy was performed to fit segments **1a**, **1b**, and their combinations, respectively (see the Supporting Information). As a consequence, the fitting of 17 experimental RDCs extracted from **1a** and **1b** (C1–H-1 to C29–H-29; Figures S9–S11, Table S11) to the DFT-optimized structures, led to possible relative configurations, of which the 2*R**,4*S**,5*R**,6*R**,12*R**,14*R**,15*S**,16*S**,19*S** configuration had the best fitting, showing the lowest *Q* factor of 0.053 (Figure S10), which agreed with the *J*-couplings and NOE NMR-based configurational analyses. The absolute configuration of **1** (substructures **1a** and **1b**) was determined by the modified Mosher method. Treatment of **1** with (*R*)- and (*S*)-MTPA chloride in anhydrous pyridine provided the corresponding (*S*)- and (*R*)-MTPA esters **1d** and **1e** (Figure S12, Table S14), which unequivocally pinpointed the 2*R*,4*S*,5*R*,6*R*,12*R*,14*R*,15*S*,16*S*,19*S* configuration of **1**. However, determining the absolute configurations of the stereocenters in substructure **1c** was challenging, owing to the deficiency of a functionalizable group (e.g., hydroxy group) in this flexible chain, as well as their remote location from the core structure. This problem was successfully circumvented by the liberation of methyl (*Z*)-3-(3-(2-hydroxypropyl)oxiran-2-yl)acrylate (**1f**) upon the alkaline hydrolysis of **1** as detailed in the Supporting Information. To the best of our knowledge, the releasable **1f** remained a new chemical entity, which motivated us to synthesize all four possible stereoisomers, including (22*R*,24*R*,25*S*)-**1g**, (22*R*,24*S*,25*R*)-**1h**, (22*S*,24*R*,25*S*)-**1i**, and (22*S*,24*S*,25*R*)-**1j** (Figure 3; for details, see the Supporting Information). With the authentic samples in hand, their ¹H NMR spectra comparison and HPLC analysis on a chiral stationary phase

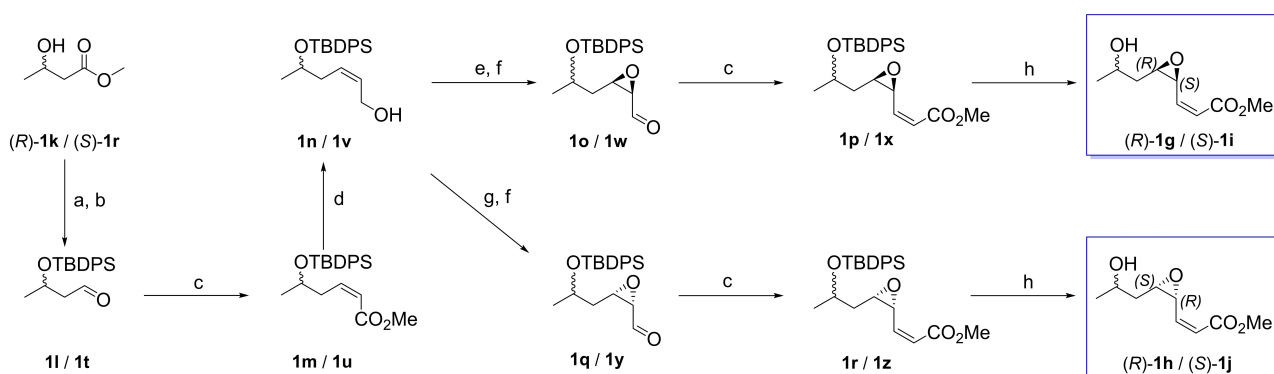


Figure 3. Chemical synthesis of four stereoisomers of the new entity **1f**: a) TBDPSCl, imidazole, DMF, 0 °C–rt; b) DIBAL-H, −78 °C; c) (CF₃CH₂O)₂P(O)CH₂CO₂Me, KHMDS, 18-crown-6; d) DIBAL-H, −78 °C; e) Ti(Oi-Pr)₄, TBHP, L-(+)-DIPT; f) DMP, NaHCO₃; g) Ti(Oi-Pr)₄, TBHP, D-(−)-DIPT; h) TBAF, HOAc, room temperature. DIBAL-H = diisobutylaluminum hydride, DIBT = diisopropyl tartrate, DMF = *N,N*-dimethylformamide, DMP = Dess–Martin periodinane, KHMDS = potassium bis(trimethylsilyl)amide, TBAF = tetrabutylammonium fluoride, TBDPS = *tert*-butyldiphenylsilyl, TBHP = *tert*-butyl hydroperoxide.

with that of **1f** liberated from **1**, demonstrated that the stereoisomer (2*R*,2*S*,2*S**R*)-**1h** exactly matched **1f** (Figure S15). Taken together, the absolute configuration of **1** was ultimately established as 2*R*,4*S*,5*R*,6*R*,12*R*,14*R*,15*S*,16*S*,19*S*,22*R*,24*S*,25*R*.

Tricrilactone B (**2**) was demonstrated to possess a molecular formula of C₂₁H₂₈O₈ from the Na⁺-liganded molecular ion at *m/z* 431.1676 (calcd for C₂₁H₂₈O₈Na, 431.1676) in its HR-ESI-MS. The ¹H and ¹³C NMR spectra of **2** revealed two olefins and two ester carbonyls accounting four of its eight degrees of unsaturation. Scrutinizing its 1D and 2D NMR spectra (COSY, HMQC and HMBC) of **2** disclosed the existence of a 10-membered macrolide moiety (C1–C10) identical to that in **1** (Table S3). However, the obvious difference was that a pair of 1,2-disubstituted double bond resonances at δ_H 6.28 (dd, *J*=6.0, 1.5 Hz) and 5.96 (dd, *J*=6.0, 2.2 Hz). The small coupling constant (*J*_{H₆,H₇}=6.0 Hz), coupled with two downfield shifted carbon signals resonating at δ_C 91.5 and 126.2, suggested the existence of an ether bridge between C5 and C8, thus leading to the formation of a dihydrofuran ring. Moreover, a pair of mutually coupled proton signals at δ_H 2.40 and 2.64 ascribable to a methylene group exhibited the HMBC correlations with C8, C10, C18, and C20 (Figure S16), which unraveled a 10-membered macrolide-derived homodimer featuring a methylene-tethered linkage. The structural proposal was substantiated by the single-crystal X-ray diffraction (Cu Kα),^[17] which facilitated the establishment of an unconventional 9/5/6/6-fused tetracyclic macrolide with a rare 1,5-dioxonan-2-one nucleus, simultaneously pinpointing its 2*R*,4*S*,5*S*,8*S*,9*R*,12*R*,16*R* configuration (Figure 4).

Tricrilactone C (**3**) displayed the same molecular formula (C₂₁H₂₈O₈) as that of **2** according to the Na⁺-liganded molecular ion at *m/z* 431.1676 (calcd for C₂₁H₂₈O₈Na, 431.1676) in its HR-ESI-MS. The ¹H and ¹³C NMR data of **3** (Table S3) bore a close resemblance to those of **2**, indicating that **3** could be a stereoisomer of **2**. This proposal was confirmed by its 1D and 2D NMR spectra, which allowed

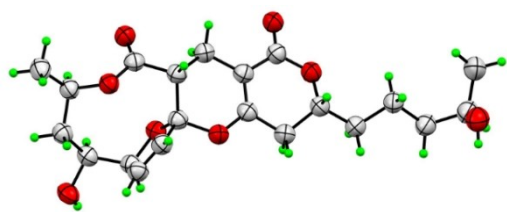


Figure 4. X-ray structure of **2**.

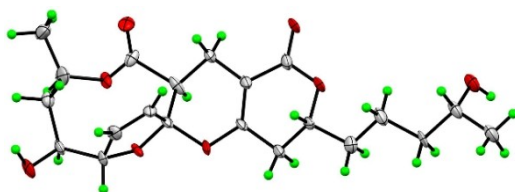


Figure 5. X-ray structure of **3**.

the unambiguous assignment of all the ¹H and ¹³C NMR signals. However, the upfield shift of C7 (Δδ up to −5.0 ppm), arising from the γ-steric compression effect of the methylene group,^[18] suggested that **3** was the 9-epimer of **2**. This assumption was supported by the single crystal X-ray diffraction (Cu Kα), which revealed that **3** possessed a 2*R*,4*S*,5*S*,8*S*,9*S*,12*R*,16*R* configuration (Figure 5).

Tricrilactone D (**4**) was analyzed to have a molecular formula of C₂₁H₂₄O₈ by its HR-ESI-MS giving the Na⁺-liganded molecular ion at *m/z* 427.1363 (calcd for C₂₁H₂₄O₈Na, 431.1363). In other words, it possessed two extra degrees of unsaturation in comparison to that of **2**. The ¹H and ¹³C NMR spectra of **4** were very similar to those of **2**, the signals attributable to a *cis*-1,2-disubstituted double bond at δ_H 5.66/δ_C 133.9 and δ_H 5.94/δ_C 126.1 were excluded (Table S4). This observation, along with a set of COSY correlations of CH₃-1/H-2/H₂-3/H-4/H-5/H-6/H-7 and CH₃-11/H-12/H-13/H-14/H-15/H-16/H-17 (Figure S16), suggested that **4** might share an identical framework with that of **2** and **3**. However, the clear HMBC correlations of H-12 with C20, H-16 with C18, and H-17 with C19 highlighted that an additional 10-membered macrocycle instead of a δ-lactone was incorporated in **4**. Surprisingly, a *cis*-14,15-epoxide ring was confirmed by the HMBC correlations of H-14 with C16 and H-15 with C17, leading to the construction of an undescribed 9/5/6/10/3-fused pentacyclic ring skeleton (Figure 1). Despite our efforts, we could grow no crystals suitable for X-ray analyses of **4**. However, the NOE correlations of H₃-1/H-3a/H-6/H-7/H-9 and H-2/H-4/H-3b/H-5 observed from **4** are very similar to those of **2** and **3** (Figure S17), whose configurations were confirmed by the single-crystal X-ray diffraction (Figures 2 and 3). This observation indicated that they might share the same (2*R**,4*S**,5*S**,8*S**,9*R**)-configuration. Meanwhile, the NOE correlations of H-12/H-14/H-15 allowed for the assignment of its (12*R**,14*S**,15*R**)-configuration, which was compatible with that of **1** (Figure 2). The above assumptions were supported by the ¹³C NMR chemical-shift calculations of **4** (Table S15), based on a high correlation coefficient (*R*²) of 0.999 (Figure S18, Table S16). The absolute configuration of **4** was determined by the modified Mosher method (Figure S12, Table S17), which was independently validated by the calculated electronic circular dichroism (ECD) spectrum of **4** (Figure S19), collectively establishing its (2*R*,4*S*,5*S*,8*S*,9*R*,12*R*,14*S*,15*R*)-configuration.

Tricrilactone E (**5**) was found to have a molecular formula of C₂₂H₃₀O₈ corresponding to its Na⁺-liganded molecular ion at *m/z* 445.1833 in its HR-ESI-MS (calcd for C₂₂H₃₀O₈Na, 445.1833). In other words, it might be compound **2** with an extra methyl group. The assumption was further evidenced by the ¹H NMR spectrum of **5** (Table S5), where a doublet at δ_H 1.25 (d, *J*=6.6 Hz) showed HSQC correlation with the carbon signal at δ_C 19.7. The unchallengeable designation of all ¹H and ¹³C NMR data of **5** was substantiated by 2D NMR experiments (HSQC, COSY, and HMBC), leading to the construction of its planar structure edited by a methyl group on the 3,4-dihydro-2*H*-pyran ring (Figure 1). In this molecule, the key HMBC correlation indicating the δ-lactone could not be observed between H-

16 and C20 identical to that in **2**, probably due to the highly deshielded C20 ester carbon atom. Nevertheless, the ester bond was next reinforced by the ^{13}C NMR experiments for **5** in CD_3OD and a $\text{CD}_3\text{OD}/\text{CD}_3\text{OH}$ mixture (1:1) (Figure 6), because its single crystals could not be obtained after many attempts. The results showed that the carbon peak of C12 instead of C16 was broadened (Figure 6), owing to the carbon signals located at the β -position of an exchangeable protons being doubled or broadened in a mixture of $\text{CD}_3\text{OD}/\text{CD}_3\text{OH}$ (1:1) by a β -isotope effect.^[19] This outcome consolidated our elucidated structure of **5**. The relative configuration of **5** was accommodated by the interpretation of its NOESY spectrum (Figure S17). The NOE correlations of $\text{H}_3\text{-}22/\text{H-}9/\text{H-}7/\text{H-}6/\text{H-}3\text{a}/\text{H}_3\text{-}1$ and $\text{H-}2/\text{H-}4/\text{H-}3\text{b}/\text{H-}5$ of **5** bear close resemblance to those of **2-4**, whose configurations were assigned by single-crystal X-ray diffraction (Figures 4 and 5) and ^{13}C NMR calculations (Figure S18). This information, along with the similar chemical shifts of **5** (for C1–C10) to those of **2-4**, suggested that it might possess the $2R^*,4S^*,5S^*,8S^*,9R^*,21R^*$ configuration, which was supported by the ^{13}C NMR calculation (Figure S20). The $2R,4S,5S,8S,9R,21R$ configuration was determined by the modified Mosher method, simultaneously assigning the stereochemical configuration of C12 as *R* (Figure S12, Table S18). However, the only missing information was the configuration at C16. To settle this problem, the ^{13}C NMR calculation method was utilized to discriminate two possible truncated models, namely $(2R,4S,5S,8S,9R,16R,21R)$ -**5A** and $(2R,4S,5S,8S,9R,16S,21R)$ -**5B** (Figure S20, Tables S19–S21), which was examined by the customizable DP4+ method (Table S22).^[20] The results showed a 99.82 % probability for **5A** and 0.18 % probability for **5B** on the basis of the ^1H and ^{13}C NMR data, which was underpinned by the calculated ECD spectrum of **5** (Figure S21), allowing

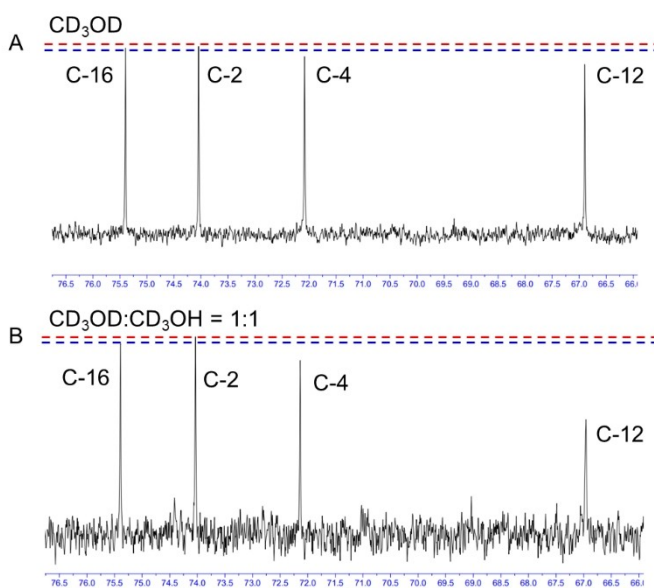


Figure 6. ^{13}C NMR spectra of **5** in A) CD_3OD and B) $\text{CD}_3\text{OD}/\text{CD}_3\text{OH}$ (1:1).

its absolute configuration to be explicitly assigned as $2R,4S,5S,8S,9R,12R,16R,21R$.

Tricrilactone F (**6**) was evidenced to have a molecular formula of $\text{C}_{22}\text{H}_{30}\text{O}_9$ from the Na^+ -liganded molecular ion at m/z 461.1782 in its HR-ESI-MS (calcd for $\text{C}_{22}\text{H}_{30}\text{O}_9\text{Na}$, 461.1782), allowing one extra O to be added in comparison to that of **5** (Table S6). In the ^{13}C NMR spectrum, the signal at δ_{C} 34.4 in **5** was replaced by an oxygenated signal at δ_{C} 72.3 in **6**. The observation indicated that compound **6** was a 15-hydroxylated derivative of **5**. This assumption was confirmed by its 2D NMR spectra (COSY, HSQC and HMBC), which allowed the ascription of all ^1H and ^{13}C NMR signals. Specifically, validating the existence of a δ -lactone moiety seemed to be challenging, owing to the absence of the HMBC correlation from H-16 to C20. Hence, the following ^{13}C NMR experiments for **6** in CD_3OD and a $\text{CD}_3\text{OD}/\text{CD}_3\text{OH}$ mixture (1:1) (Figure S22) were performed to tackle this problem. The results revealed that both the C12 and C15 signals were broadened, whereas the C16 peak was not affected, suggesting that C12 and C15 were individually connected to the free OH groups. Interpretation of the NOE correlations and coupling constants (Figure S17, Table S6), in combination with the analysis of its (*S*-) and (*R*-) tris-Mosher esters, assigned a $2R,4S,5S,8S,9R,12R,15S,21R$ configuration by the signs of $\Delta\delta^{SR}$ values proposed for the 1,4-diol systems (Figure S12, Table S23).^[21] The remaining stereocenter of C16 was subjected to the ^{13}C NMR calculation by discriminating two truncated models, $(2R,4S,5S,8S,9R,15S,16R,21R)$ -**6A** and $(2R,4S,5S,8S,9R,15S,16S,21R)$ -**6B** (Figure S23, Tables S24–S26), followed by examination by the customizable DP4+ method (Table S27). The results showed a 100 % probability for **6A** based on the ^1H and ^{13}C NMR data, which was further verified by the ECD calculation (Figure S24), unequivocally pinpointing its $2R,4S,5S,8S,9R,12R,15S,16R,21R$ configuration.

Tricrilactone G (**7**), isolated as a colorless block, gave a $[\text{M}+\text{H}]^+$ ion peak at m/z 506.2385 in its HR-ESI-MS spectrum, suggesting its molecular formula to be $\text{C}_{26}\text{H}_{35}\text{NO}_9$ (calcd for $\text{C}_{26}\text{H}_{35}\text{NO}_9$, 506.2385). Inspection of the ^1H and ^{13}C NMR spectra of **7** (Table S7) indicated that it harbored two 10-membered macrolide subunits identical to that of **1**. This speculation was ascertained by two sets of sequential COSY correlations of $\text{H}_3\text{-}1/\text{H-}2/\text{H}_2\text{-}3/\text{H-}4/\text{H-}5/\text{H-}6/\text{H-}7$ and $\text{H}_3\text{-}11/\text{H-}12/\text{H}_2\text{-}13/\text{H-}14/\text{H-}15/\text{H-}16/\text{H}_2\text{-}17$, as well as the key HMBC correlations of H-2 with C10, and of H-12 with C20. Additionally, the COSY correlations of $\text{H}_3\text{-}21/\text{H-}22/\text{H-}23$, and the HMBC correlations of $\text{H}_3\text{-}21$ with C23, of H-22 with C24, of H-23 with C25, and of $\text{H}_3\text{-}26$ with C24 (Figure S16), suggested the presence of a 2,3,3-trisubstituted (*E*)-hex-4-ene residue. The three defined substructures were then pieced together through the HMBC correlations of H-7 with C25, of H-23 with C7, of H-6 with C24, and of H-16 with C6 and C25, leading to the construction of a new class of pyrrolidine-containing macrolide-alkaloid hybrid incorporating an unparalleled bridged azatricyclic framework. Finally, tricrilactone B (**7**) was crystallized from a *n*-hexane/ethanol/water (10:10:1) solution at 4°C. The architecture of **7** was further confirmed by single-crystal X-ray diffraction (Cu

K α), which underscored simultaneously its 2*R*,4*S*,5*R*,6*S*,7*R*,12*R*,14*S*,15*R*,16*S*,24*S*,25*S* configuration (Figure 7).

Tricrilactone H (**8**) has a molecular formula of C₂₀H₂₆O₇ based on the Na⁺-liganded molecular ion at *m/z* 401.1576 in its HR-ESI-MS (calcd for C₂₀H₂₆O₇Na, 401.1576). The ¹H NMR spectrum displayed a pair of mutually coupled proton signals at δ_{H} 5.78 (dd, *J* = 12.5, 4.5 Hz) and 6.30 (dd, *J* = 12.5, 2.4 Hz; Table S8), suggesting the presence of a *cis*-1,2-disubstituted double bond.

In the ¹³C NMR spectrum, the signals at δ_{C} 198.0, 133.4 and 133.4 indicated an α,β -unsaturated ketone unit, while the signals at δ_{C} 167.4 and 166.3 highlighted the existence of two ester motifs in the molecule. Detailed analysis of its 2D NMR spectra (COSY, NOESY, HSQC and HMBC) enabled the exact assignment of all ¹H and ¹³C NMR data of **8**, leading to the establishment of a unique bridged bicyclic skeleton furnished by forming a unique C6–C19 linkage. Compound **8** was ascertained to have a 2*R*,6*R*,12*R*,14*S*,15*R*,19*R* configuration by single-crystal X-ray diffraction (Cu K α ; Figure 7).

The structural features of tricrilactones A–H (**1–8**) facilitated our supposition that they might originate from a new building block, (*Z*)-3-methyl-4,11-dioxabicyclo-[8.1.0]undec-8-ene-5,7-dione. To validate the postulation, LC–MS guided isolation resulted in the characterization of a new compound, dubbed protilactone A, from a 7 day fermentation of the fungus. The structure of protilactone A was identified by its 1D (Table S9) and 2D NMR spectra, as well as single-crystal X-ray diffraction (Cu K α) of the corresponding hydrazone (Figure S25). To our surprise, this molecule was decorated with a *cis* double bond, which is a rare phenomenon in the family of 10-membered macrolides.^[7] Concurrently, a crucial, but very unstable and insoluble intermediate, named protilactone B, was also obtained. Its structure was discerned by the characteristic ¹H and ¹³C NMR resonances (Table S10) reminiscent of the tricrilactone A (**1**) core scaffold. Subsequent analysis of its 2D NMR data confirmed our conjecture of the structure. The formulated configuration of protilactone B was collectively assumed by its NOESY spectrum and the ¹³C

NMR calculation (Figure S26, Tables S28 and S29), as well as the biogenetic consideration of the family of macrolides. Nevertheless, crystals of protilactone B failed to be detected owing to the insolubility and instability of the sample.

Methylene-bridged dimers are infrequently encountered in natural products. However, more than 100 natural compounds with such a feature have been characterized from plants and microorganisms.^[22] Tricrilactones B–D (**2–4**) comprise a bridging methylene carbon atom (C21), which is unaccountable for in the monomeric unit, indicating that a one-carbon (C1) building block is involved in the molecule. To our knowledge, *S*-adenosyl methionine and formaldehyde are the two most common C1 units in nature.^[22,23] Thus, it is likely that *S*-adenosyl methionine or formaldehyde could be the source of methylene carbon atom (C21) in compounds **2–4**. To test this hypothesis, two independent experiments were performed. Initially, *Trichocladium crispatum* was regrown with the addition of [Me-*d*₃]-methionine. The fungal culture was extracted, followed by LC-ESI-MS analysis. However, no [Me-*d*₃]-methionine could be introduced into any of the compounds **2–4**. Given that some fungi are capable of producing formaldehyde through direct oxidation of sarcosine or methanol,^[24] we conducted the isotope-labeling experiment using [D₄]-methanol. To our surprise, the deuterated compounds **2–4** were generated with the corresponding [M+H]⁺ ions at *m/z* 411 (**2** and **3**; Figures S27 and S28) and 407 (**4**; Figure S29), respectively, showing a 2 Da increment from that of **2–4** without exposure to [D₄]-methanol. This observation demonstrated that the methylene carbon atoms (C21) of **2–4** are derived from methanol, which would be oxidized to formaldehyde and then triggered the dimerization of monomeric precursor **11** to generate tricrilactones B–D (**2–4**). Since the formaldehyde-induced dimerization in natural products is a non-enzymatic process in most cases,^[22,25] protilactone A was therefore treated with formaldehyde aqueous solution under the physiological conditions. A methylene-bridged dimer was obtained (see the Supporting Information), suggesting that the coupling between protilactone A and formaldehyde could occur without an enzyme during the biosynthesis of **2–4** in the fungal cells. Formaldehyde is well-known for its toxicity against various fungi;^[24] hence, the formaldehyde-triggered dimerization reactions could be a new strategy for self-detoxification of fungi that needs further investigation. To the best of our knowledge, this is the first report of formaldehyde-induced macrolide dimers from nature.

With respect to tricrilactone G (**7**), the unusually fused pyrrolidine motif might originate from (*E*)-2-aminohex-4-en-3-one, whose nitrogen atom was predicted to be derived from alanine. To reinforce this assumption, *Trichocladium crispatum* was recultured in the presence of [1-¹⁵N]-alanine, and the extract was subjected to LC-ESI-MS analysis, which exhibited an obviously increased abundance of ¹⁵N corresponding to its [M+H]⁺ ion peak at *m/z* 507 (Figure S30), suggesting the incorporation of an alanine residue in the biosynthesis of **7**. Based on these intermediate-trapping and isotopic labeling experiments, a putative biosynthetic path-

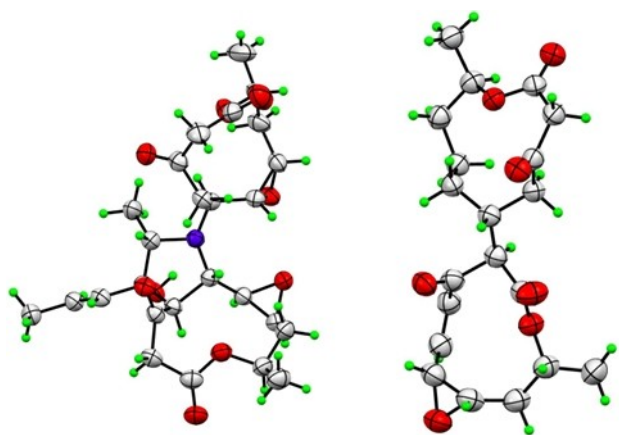


Figure 7. X-ray structures of **7** (left) and **8** (right).

way involving (*Z*)-3-methyl-4,11-dioxabicyclo[8.1.0]undec-8-ene-5,7-dione, formaldehyde, and alanine was proposed for **1–4** and **7** (see the Supporting Information).

Zebrafish have emerged as a reliable vertebral model for the evaluation of human disease, because of the high levels of genetic and functional homology between zebrafish and humans.^[26] This observation, together with the medicative macrodiolides for osteoporosis,^[27] spurred us to evaluate **1–7**, but not **8** (owing to scarcity of the sample), for their antiosteoporotic activity on dexamethasone-induced osteoporotic zebrafish.^[28] All of the tested compounds were shown to alleviate bone loss in osteoporotic zebrafish at 0.4, 2.0, and 10.0 μM , in a dose-dependent fashion (Figure S31), and were thus more potent than the positive control, alendronate, a clinically used antiosteoporosis drug.^[29] Notably, compounds **5** and **6** exhibited the most potent therapeutic effects at 0.4 μM , bearing comparison with alendronate at 10.0 μM (Figure S31).

As osteoporosis is characterized by an imbalance between bone resorption and bone formation, current drugs for osteoporosis either inhibit bone resorption, or stimulate bone formation.^[30] Alkaline phosphatase (ALP) and tartrate resistant acid phosphatase (TRAP) are two biomarkers during osteoporosis, with the former reflecting osteoblast differentiation (bone formation), and the latter embodying the activity of osteoclast (bone resorption).^[31] To learn the mechanism for the antiosteoporosis action of tricyclactones on zebrafish, we assessed the quantities of these two markers.

As depicted in Figure 8, dexamethasone (DXM) could induce an obvious decrease in ALP, and simultaneously an apparent increase in TRAP as compared to the control group, thus leading to osteoporosis (Figure 8B). To our surprise, treatment with tricyclactone G (**7**) significantly reversed the amounts of ALP and TRAP, with a comparable moderating effect to that of alendronate, suggesting the restoration of bone formation–resorption homeostasis (Fig-

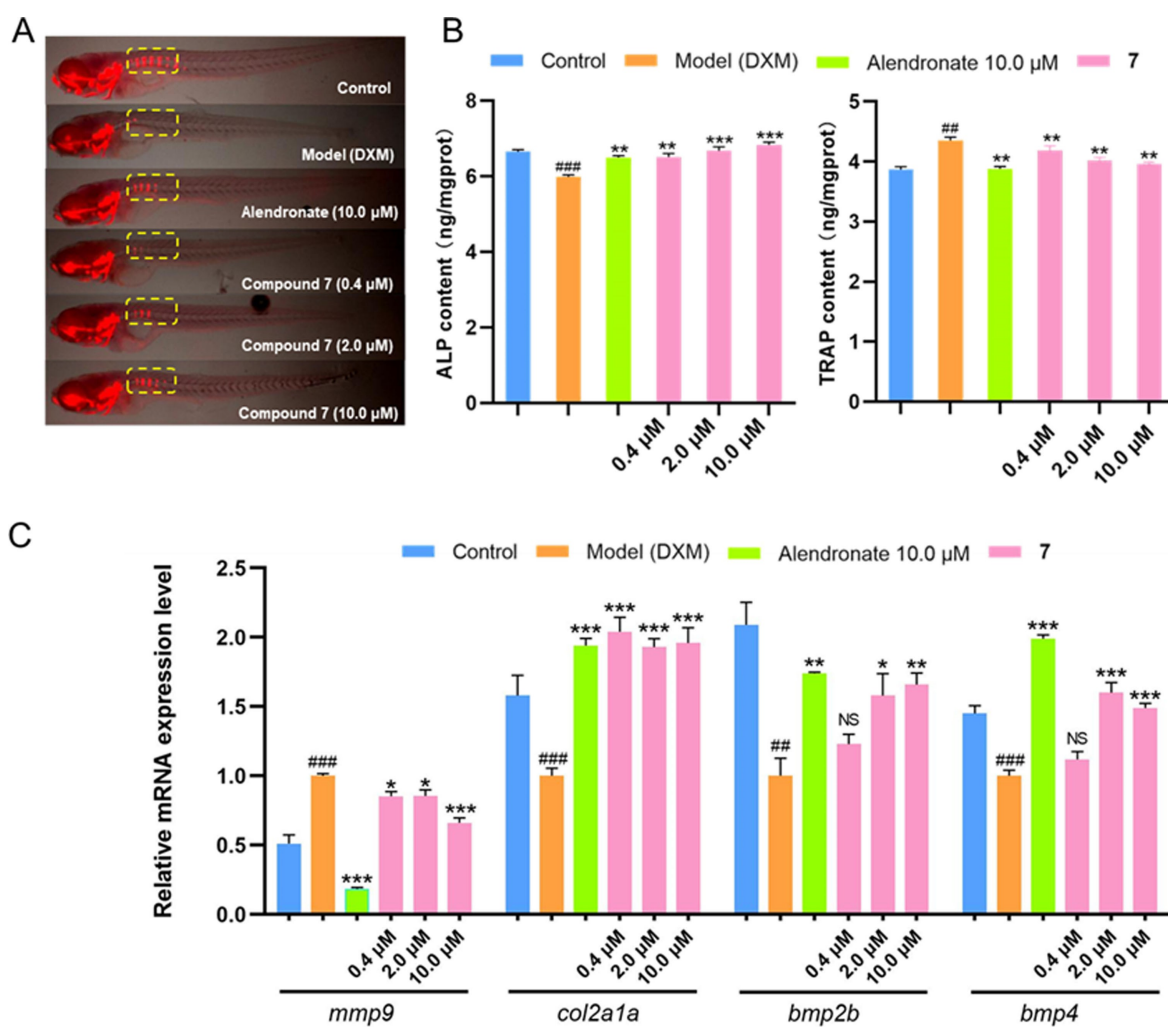


Figure 8. Evaluation of antiosteoporosis effect of compound **7** in zebrafish. A) Representative images of zebrafish treated with 0.4, 2.0 and 10.0 μM of **7**. The yellow dotted box denotes the analyzed region. B) Effect of **7** on ALP and TRAP contents. C) Effect of **7** on relative mRNA expression level corresponding to four genes *mmp9*, *col2a1a*, *bmp2b*, and *bmp4*. All values are expressed as means \pm SD. Compared with a control group (DMSO), ##P < 0.01, ###P < 0.001. Compared with the model group (DXM), *P < 0.05, **P < 0.01, ***P < 0.001, NS: nonsignificant (P > 0.05).

ure 8B). Subsequently, we examined whether the expression levels of genes specifically regulating bone development were changed. We initially detected the expression of bone-specific marker genes *col2ala* and *mmp9*. The former is a type II collagen synthase related to periosteal ossification and endochondral bone morphogenesis,^[30] whereas the latter is a member of the matrix metalloproteinase family that can degrade collagens.^[32] Quantitative PCR (qPCR) analysis revealed that administration of **7** dramatically up-regulated *col2ala* expression, which was comparable to the positive control, alendronate. However, the transcriptional level of *mmp9* was clearly decreased as compared to dexamethasone-treated zebrafish (Figure 8C). Moreover, we also detected the mRNA levels of *bmp2b* and *bmp4*, two members of bone morphogenetic proteins that induce the formation of bone and cartilage.^[30,33] Results showed that the expression levels of *bmp2b* and *bmp4* were both significantly enhanced in a roughly dose-dependent manner after treatment of **7** (Figure 8C). The data showed that tricyclactones may ameliorate osteoporosis by remodeling the balance between bone formation and bone resorption, and simultaneously promoting cartilage and skeletal development. Further investigation is still necessary to explore the therapeutic effect on osteoporosis of tricyclactones.

Interestingly, we found that **6** was also cytotoxic against the tested cancer cells (A549, SW480 and MDA-MB-231; Table S30), with IC₅₀ values of 5.39, 8.24, and 6.79 μM, respectively. In addition, **6** could induce apoptosis of these cancer cells (Figure S32), presumably by disrupting the mitochondrial membrane potential (Figure S33). Thus, the therapeutic window of **6** for osteoporosis might be very low, due to its potential cytotoxicity. Meanwhile, none of the remaining compounds showed cytotoxicity at 20.0 μM. However, understanding the width of the therapeutic window for these tricyclactones is still essential for developing safe and effective antiosteoporosis drugs.

Conclusion

In summary, we have described the full characterization of a family of novel tricyclactone macrolides with potent antiosteoporotic activity from *Trichocladium crispatum*. The study also provides evidence for the involvement of formaldehyde, alanine, and (*Z*)-3-methyl-4,11-dioxabicyclo-[8.1.0]undec-8-ene-5,7-dione in the biosynthesis of these macrolides, as based on intermediate-trapping and isotope-feeding experiments. Collectively, this family of tricyclactones represents five distinctive ring skeletons and in particular the first-time characterization of formaldehyde-induced and pyrrolidine-containing microbial macrolide dimers from nature. Interestingly, formaldehyde-triggered non-enzymatic reactions could be a new strategy for self-detoxification of fungi^[24] and the construction of sophisticated structures with remarkable bioactivities.^[22] It is enticing to use this type of dimeric reaction to access valuable bioactive natural products due to its simplicity, eco-friendliness, and high efficiency.^[34] Furthermore, these potent antiosteoporosis architectures may not only play an impor-

tant role in the discovery of new lead compounds for the treatment of osteoporosis, but may also inspire chemists to synthesize medium-sized lactones,^[6b] and they open the interesting topic of the discovery and characterization of more fungal macrocyclases involved in the formation of 10-membered lactones.^[35]

Acknowledgements

This research was supported by the National Natural Science Foundation of China (22277099, 82173714, 22077102). We thank Dr. Xiuhuan Li (State Key Laboratory of Crop Stress Biology for Arid Areas, NWFU) for NMR experimental assistance and Lu-Qi Li (Life Science Research Core Services, NWFU) for HRESIMS data analysis.

Conflict of Interest

The authors declare no conflict of interest.

Data Availability Statement

The data that support the findings of this study are available in the Supporting Information of this article.

Keywords: Antiosteoporosis · Fungal Natural Products · Isotope Labeling · Macrolides · Structure Elucidation

- [1] J. E. Compston, M. R. McClung, W. D. Leslie, *Lancet* **2019**, 393, 364–376.
- [2] K. E. Ensrud, C. J. Crandall, *Ann. Intern. Med.* **2017**, 166, ITC17–32.
- [3] J. Huo, Y. Ding, X. Wei, Q. Chen, B. Zhao, *J. Biochem. Mol. Toxicol.* **2022**, e23209.
- [4] a) G. Adami, A. Fassio, D. Gatti, O. Viapiana, C. Benini, M. I. Danila, K. G. Saag, M. Rossini, *Ther. Adv. Musculoskelet. Dis.* **2022**, 14, 1–14; b) S. Wang, Y. Yuan, Q. Lin, H. Zhou, B. Tang, Y. Liu, H. Huang, B. Liang, Y. Mao, K. Liu, X. Shi, *Front. Pharmacol.* **2022**, 13, 937538.
- [5] H. Wang, L. Yang, J. Chao, *Front. Endocrinol.* **2022**, 13, 932488.
- [6] a) A. Evidente, *Nat. Prod. Rep.* **2022**, 39, 1591–1621; b) I. Shiina, *Chem. Rev.* **2007**, 107, 239–273.
- [7] V. B. Riatto, R. A. Pilli, M. M. Victor, *Tetrahedron* **2008**, 64, 2279–2300.
- [8] J. Liu, A. Liu, Y. Hu, *Nat. Prod. Rep.* **2021**, 38, 1469–1505.
- [9] M. J. Ackland, J. R. Hanson, P. B. Hitchcock, R. P. Mabelis, A. H. Ratcliffe, *J. Chem. Soc. Perkin Trans. 1* **1984**, 2755–2757.
- [10] X. Li, H. P. Chen, L. Zhou, J. Fan, T. Awakawa, T. Mori, R. Ushimaru, I. Abe, J. K. Liu, *Org. Lett.* **2022**, 24, 8627–8632.
- [11] a) W. B. Han, G. Y. Wang, J. J. Tang, W. J. Wang, H. Liu, R. R. Gil, A. Navarro-Vázquez, X. Lei, J. M. Gao, *Org. Lett.* **2020**, 22, 405–409; b) H. Y. Tang, Q. Zhang, Y. Q. Gao, A. L. Zhang, J. M. Gao, *RSC Adv.* **2015**, 5, 2185–2190.
- [12] K. Tori, T. Nakagawa, T. Komeno, *J. Org. Chem.* **1964**, 29, 1136–1141.
- [13] W. Koźmiński, D. Nanz, *J. Magn. Reson.* **1997**, 124, 383–392.

- [14] G. W. Li, H. Liu, F. Qiu, X. J. Wang, X. X. Lei, *Nat. Prod. Bioprospect.* **2018**, *8*, 279–295.
- [15] A. Enthart, J. C. Freudenberger, J. Furrer, H. Kessler, B. Luy, *J. Magn. Reson.* **2008**, *192*, 314–322.
- [16] X. Lei, F. Qiu, H. Sun, L. Bai, W. X. Wang, W. Xiang, H. Xiao, *Angew. Chem. Int. Ed.* **2017**, *56*, 12857–12861; *Angew. Chem.* **2017**, *129*, 13037–13041.
- [17] Deposition numbers 2219597 (compound **2**), 2219593 (compound **3**), 2219570 (compound **7**), 2219574 (compound **8**), and 2219573 (compound **11a**) contain the supplementary crystallographic data for this paper. These data are provided free of charge by the joint Cambridge Crystallographic Data Centre and Fachinformationszentrum Karlsruhe Access Structures service.
- [18] D. W. Brooks, H. Mazdiyasi, P. G. Grothaus, *J. Org. Chem.* **1987**, *52*, 3223–3232.
- [19] P. G. Williams, R. N. Asolkar, T. Kondratyuk, J. M. Pezzuto, P. R. Jensen, W. Fenical, *J. Nat. Prod.* **2007**, *70*, 83–88.
- [20] M. M. Zanardi, A. M. Sarotti, *J. Org. Chem.* **2021**, *86*, 8544–8548.
- [21] F. Freire, J. M. Seco, E. Quiñoá, R. Riguera, *J. Org. Chem.* **2005**, *70*, 3778–3790.
- [22] Y. Fan, J. Shen, Z. Liu, K. Xia, W. Zhu, P. Fu, *Nat. Prod. Rep.* **2022**, *39*, 1305–1324.
- [23] L. Colombo, C. Gennari, G. S. Ricca, C. Scolastico, F. Aragozzini, *J. Chem. Soc. Chem. Commun.* **1981**, 575–576.
- [24] R. Himstedt, S. Wagner, R. J. R. Jaeger, M.-L. L. Watat, J. Backenköhler, Z. Rupic, M. Stadler, P. Spiteller, *ChemBioChem* **2020**, *21*, 1613–1620.
- [25] L. M. Bouthillette, V. Aniebok, D. A. Colosimo, D. Brumley, J. B. MacMillan, *Chem. Rev.* **2022**, *122*, 14815–14841.
- [26] M. Ceci, V. Mariano, N. Romano, *Rev. Neurosci.* **2018**, *30*, 45–66.
- [27] a) T. T. Wang, Y. J. Wei, H. M. Ge, R. H. Jiao, R. X. Tan, *Org. Lett.* **2018**, *20*, 1007–1010; b) T. T. Wang, Y. J. Wei, H. M. Ge, R. H. Jiao, R. X. Tan, *Org. Lett.* **2018**, *20*, 2490–2493.
- [28] D. J. M. Bergen, E. Kague, C. L. Hammond, *Front. Endocrinol.* **2019**, *10*, 6.
- [29] A. Villanueva-Martínez, L. Hernández-Rizo, A. Ganem-Rondero, *Int. J. Pharm.* **2020**, *582*, 119312.
- [30] W. Peng, W. Zhang, Q. Wu, S. Cai, T. Jia, J. Sun, Z. Lin, G. Alitongbieke, Y. Chen, Y. Su, J. Lin, L. Cai, Y. Sun, Y. Pan, Y. Xue, *J. Nat. Prod.* **2021**, *84*, 1294–1305.
- [31] H. Yin, S. Wang, Y. Zhang, M. Wu, J. Wang, Y. Ma, *Biomed. Pharmacother.* **2018**, *97*, 995–999.
- [32] Y. Zhang, H. Huang, G. Zhao, T. Yokoyama, H. Vega, Y. Huang, R. Sood, K. Bishop, V. Maduro, J. Accardi, C. Toro, C. F. Boerkoel, K. Lyons, W. A. Gahl, X. Duan, M. C. Malicdan, S. Lin, *PLoS Genet.* **2017**, *13*, e1006481.
- [33] K. Miyazono, Y. Kamiya, M. Morikawa, *J. Biochem.* **2010**, *147*, 35–51.
- [34] Z. Liu, S. Yin, R. Zhang, W. Zhu, P. Fu, *ACS Sustainable Chem. Eng.* **2022**, *10*, 655–661.
- [35] D. W. Gao, C. S. Jamieson, G. Wang, Y. Yan, J. Zhou, K. N. Houk, Y. Tang, *J. Am. Chem. Soc.* **2021**, *143*, 80–84.

Manuscript received: January 15, 2023

Accepted manuscript online: February 21, 2023

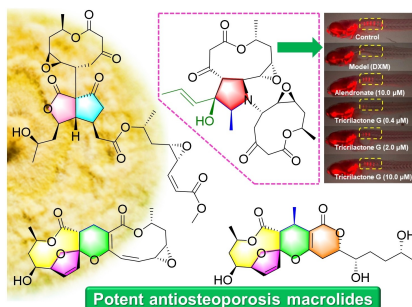
Version of record online: ■■, ■■

Research Articles

Natural Products

W.-B. Han,* Y.-J. Zhai, R. Zhang, X.-S. Gong,
J.-Q. Li, G. Xu,* X. Lei, L. Du, J.-
M. Gao* **e202300773**

Tricrilactones A–H, Potent Antiosteoporosis
Macrolides with Distinctive Ring Skeletons
from *Trichocladium crispatum*, an Alpine
Moss-Associated Fungus



A family of oligomeric 10-membered macrolides, tricrilactones A–H, was isolated from the moss-derived fungus *T. crispatum*. Intermediate-trapping and isotope labeling experiments provided evidence for their proposed biosynthetic pathway. The compounds were found to be potent antiosteoporosis agents in vivo, whereby tricrilactone G (top right-hand structure) restored bone formation-resorption homeostasis and promoted cartilage and skeletal development.